

See discussions, stats, and author profiles for this publication at: <https://www.researchgate.net/publication/7304258>

The Effect of Salt on Protein Chemical Potential Determined by Ternary Diffusion in Aqueous Solutions

ARTICLE *in* THE JOURNAL OF PHYSICAL CHEMISTRY B · FEBRUARY 2006

Impact Factor: 3.3 · DOI: 10.1021/jp054543c · Source: PubMed

CITATIONS

20

READS

18

5 AUTHORS, INCLUDING:



Onofrio Annunziata

Texas Christian University

50 PUBLICATIONS 761 CITATIONS

SEE PROFILE



Luigi Paduano

University of Naples Federico II

163 PUBLICATIONS 2,318 CITATIONS

SEE PROFILE



John Albright

Texas Christian University

71 PUBLICATIONS 906 CITATIONS

SEE PROFILE

The Effect of Salt on Protein Chemical Potential Determined by Ternary Diffusion in Aqueous Solutions

Onofrio Annunziata,^{*,†} Luigi Paduano,^{†,‡} Arne J. Pearlstein,[§] Donald G. Miller,^{†,||} and John G. Albright[†]

Department of Chemistry, Texas Christian University, Fort Worth, Texas 76129, Geosciences and Environmental Technologies, Lawrence Livermore National Laboratory, P.O. Box 808, Livermore, California 94551, Department of Mechanical and Industrial Engineering, University of Illinois at Urbana-Champaign, 1206 West Green Street, Urbana, Illinois 61801, and Dipartimento di Chimica, Università di Napoli "Federico II", Naples, 80126, Italy

Received: August 12, 2005; In Final Form: October 8, 2005

We use accurate thermodynamic derivatives extracted from high-precision measurements of the four volume-fixed diffusion coefficients in ternary solutions of lysozyme chloride in aqueous NaCl, NH₄Cl, and KCl at pH 4.5 and 25 °C to (a) assess the relative contributions of the common-ion and nonideality effects to the protein chemical potential as a function of salt concentration, (b) compare the behavior of the protein chemical potential for the three salts, which we found to be consistent with the Hofmeister series, and (c) discuss our thermodynamic data in relation to the dependence of the protein solubility on salt concentration. The four diffusion coefficients are reported at 0.6 mM lysozyme chloride and 0.25, 0.5, 0.9, 1.2, and 1.5 M KCl and extend into the protein-supersaturated region. The chemical potential cross-derivatives are extracted from diffusion data using the Onsager reciprocal relation and the equality of molal cross-derivatives of solute chemical potentials. They are compared to those calculated previously from diffusion data for lysozyme in aqueous NaCl and NH₄Cl. We estimate the effective charge on the diffusing lysozyme cation at the experimental concentrations. Our diffusion measurements on the three salts allowed us to analyze and interpret the four diffusion coefficients for charged proteins in the presence of 1:1 electrolytes. Our results may provide guidance to the understanding of protein crystallization.

Introduction

Enzymatic activity, binding of species to proteins, conformational change, and "preferential hydration"¹ are some aspects of protein behavior affected by direct interaction of proteins with either small molecules (e.g., blood gases, ligands, denaturants, precipitants)^{2,3} or other macromolecules.⁴ Thermodynamics lies at the heart of understanding these interactions. In addition, through the dependence of chemical potentials on concentration, thermodynamics is central to understanding both diffusive mass transport of proteins to and in cells, as well as active transport across cellular, nuclear, and organelle membranes.⁵

At the organ, tissue, cellular, or organelle level, in vivo systems involve very large numbers of components. Even in the laboratory, aqueous protein solutions nearly always consist of at least three components, including the solvent. Historically, thermodynamic data for such multicomponent systems have been scarce, hard to acquire, and not very precise. Lack of such data has posed significant obstacles to the development and validation of theory.

Using the first precision measurements of the full set of diffusion coefficients in a multicomponent system involving a protein,^{6–8} we have shown how to use the Onsager reciprocal relation (ORR) to extract thermodynamic data from diffusion

measurements in ternary aqueous solutions of lysozyme chloride. These include aqueous NaCl at two pH values and NH₄Cl at one of these pH values. Specifically, for each salt, we extracted the *cross-derivatives* of the protein and salt chemical potentials with respect to concentration of the other component, which we used to estimate the lysozyme chloride's "effective charge". Integration with respect to salt concentration (at constant lysozyme concentration) yielded the dependence of the lysozyme chemical potential on salt concentration, within a constant of integration.⁷

A thermodynamic basis for understanding diffusive transport in ternary lysozyme solutions is potentially important for other proteins, in reducing the current degree of empiricism in developing procedures for (a) growth of protein crystals for structural determinations^{9,10} and (b) separation of proteins from multicomponent solutions in manufacturing and research applications. In such separations, salt-induced precipitation is frequently the first step in purification of proteins from fermentation broths or from plant and animal extracts.¹¹

Here, we report diffusion and thermodynamic data for lysozyme chloride in aqueous solutions of KCl. We use these data, together with those for NaCl and NH₄Cl, to study behavior for all three salts, considered as a Hofmeister series.

In this paper, our first main objective is to provide reliable thermodynamic data that will serve as a firm thermodynamic underpinning for understanding several phenomena (including crystallization) in multicomponent protein solutions. To do this, we apply to ternary aqueous solutions of lysozyme chloride in KCl the same method⁷ for extracting thermodynamic data from

* To whom correspondence should be addressed: phone, (817) 257-6215; fax, (817) 257-5851; e-mail, O.Annunziata@tcu.edu.

[†] Texas Christian University.

[‡] Università di Napoli.

[§] University of Illinois at Urbana-Champaign.

^{||} Lawrence Livermore National Laboratory.

measured multicomponent diffusion coefficients that we previously applied in the NaCl⁷ and NH₄Cl⁸ cases. We then compare the extracted data to those of our earlier measurements for those salts, as well as to data obtained from classical equilibrium measurements, including solubility data. The precision of both our extracted data and their concentration dependence also allows us to quantitatively separate the *cross-derivatives* into contributions corresponding to the common-ion effect and nonideality. For each salt, we also estimate the “effective” protein charge and compare our values with those obtained directly from titration.

Extraction of thermodynamic data from diffusion measurements, necessarily performed away from equilibrium, has the key advantage that one can access the supersaturated region. This provides thermodynamic data in portions of the phase diagram in which traditional “direct” equilibrium measurements (e.g., of equilibrium dialysis) are extremely difficult or impossible due to precipitation. The resulting thermodynamic data are of particular interest in understanding salt-specific effects on crystallization. Moreover, our method is sensitive to protein mass concentration. This is an important advantage with respect to colligative-property measurements (e.g., vapor pressure osmometry),³ which are not directly sensitive to the typical low molar concentration of proteins.

Our second objective is to discuss the extracted thermodynamic data in relation to the effectiveness of salts in the protein precipitation process, including the Hofmeister cation series. To date, thermodynamic data relevant to the Hofmeister series have largely been limited to solubility measurements and determinations of the second virial coefficient (B_2), with their inherently limited precision. Moreover, it is known¹² that the “accessible window”¹³ of B_2 is an imperfect predictor of favorable crystallization conditions. Precise values of the derivative of the protein chemical potential with respect to salt concentration lead to the dependence of the lysozyme chemical potential itself on salt concentration. The comparison of these quantities for all three salts is consistent with the Hofmeister series of solubilities.

Our third major objective is to analyze and interpret the dependence of the four multicomponent diffusion coefficients on the nature and concentration of the salt for aqueous solutions of lysozyme chloride and NaCl, NH₄Cl, or KCl. Multicomponent diffusion effects (specifically, departures from the simple approximation of pseudo-binary diffusion) are known to be important in separation of proteins by ultrafiltration and other methods.¹⁴ Understanding the salt and concentration dependence of the diffusion coefficients (a) allows us to better understand the relative magnitudes of the diffusion coefficients and their dependence on protein charge and (b) lays the groundwork for predicting the four diffusion coefficients as functions of concentration for systems containing other 1:1 salts. The four multicomponent diffusion coefficients also allow us to estimate, for each salt, the large number of moles of salt transported with each mole of diffusing protein.

Finally, we consider some thermodynamic and crystal growth applications of the results.

The approaches demonstrated for lysozyme in aqueous solutions of these three salts are generally applicable to ternary systems in which one solute concentration greatly exceeds that of the other, as in many systems involving proteins or other biological macromolecules.⁷

Relations for Isothermal Ternary Diffusion. Diffusion can be described relative to different reference frames.¹⁵ We report isothermal diffusion coefficients for the volume- and solvent-

fixed frames. In the volume-fixed frame, the fluxes of the components of a ternary system satisfy $(J_0)_V \bar{V}_0 + (J_1)_V \bar{V}_1 + (J_2)_V \bar{V}_2 = 0$; in the solvent-fixed frame, we have $(J_0)_0 = 0$. Here, J_i and \bar{V}_i are the molar flux and partial molar volume of component i , respectively. The subscript V denotes the volume-fixed frame. The subscript 0 denotes the solvent component when appended directly to a flux and denotes the solvent-fixed frame when appended outside the parentheses to an already-subscripted flux or diffusion coefficient. Subscripts 1 and 2 refer to the protein and salt components, respectively.

Since concentration differences are small and volume changes on mixing are negligible, our measurements correspond, to an excellent approximation, to the volume-fixed frame.¹⁵ For isothermal diffusion, the matrix form of Fick’s first law in this frame in one dimension is

$$\begin{bmatrix} -(J_1)_V \\ -(J_2)_V \end{bmatrix} = \begin{bmatrix} (D_{11})_V & (D_{12})_V \\ (D_{21})_V & (D_{22})_V \end{bmatrix} \begin{bmatrix} \partial C_1 / \partial x \\ \partial C_2 / \partial x \end{bmatrix} \quad (1)$$

Here, the C_i are molar concentrations and the $(D_{ij})_V$ are volume-fixed diffusion coefficients.

The linear laws of irreversible thermodynamics for isothermal diffusion in terms of the Onsager diffusion coefficients (ODCs) $(L_{ij})_0$ are simpler in the solvent-fixed frame.^{16–18} In this frame, the fluxes for a ternary system can be written as

$$\begin{bmatrix} -(J_1)_0 \\ -(J_2)_0 \end{bmatrix} = \begin{bmatrix} (D_{11})_0 & (D_{12})_0 \\ (D_{21})_0 & (D_{22})_0 \end{bmatrix} \begin{bmatrix} \partial C_1 / \partial x \\ \partial C_2 / \partial x \end{bmatrix} = \begin{bmatrix} (L_{11})_0 & (L_{12})_0 \\ (L_{21})_0 & (L_{22})_0 \end{bmatrix} \begin{bmatrix} \partial \mu_1 / \partial x \\ \partial \mu_2 / \partial x \end{bmatrix} \quad (2)$$

where the solvent-fixed $(D_{ij})_0$ are calculated from the $(D_{ij})_V$ and \bar{V}_i ^{16–18} and μ_i is the chemical potential of the i th component. The ORR^{16–18} in the solvent-fixed frame is

$$(L_{12})_0 = (L_{21})_0 \quad (3)$$

We can use eq 2 to relate the solvent-fixed diffusion coefficients and ODCs according to

$$(D_{11})_0 = (L_{11})_0 \mu_{11} + (L_{12})_0 \mu_{21} \quad (4a)$$

$$(D_{12})_0 = (L_{11})_0 \mu_{12} + (L_{12})_0 \mu_{22} \quad (4b)$$

$$(D_{21})_0 = (L_{21})_0 \mu_{11} + (L_{22})_0 \mu_{21} \quad (4c)$$

$$(D_{22})_0 = (L_{21})_0 \mu_{12} + (L_{22})_0 \mu_{22} \quad (4d)$$

where the derivatives are defined by $\mu_{ij} \equiv (\partial \mu_i / \partial C_j)_{T,p,C_k,k \neq j}$, where T is the temperature and p the pressure.⁷

Each main-term diffusion coefficient $(D_{ii})_0$ is related to main-term (μ_{ii}) and cross-term $(\mu_{ji}, j \neq i)$ thermodynamic derivatives. For the ternary systems considered here, each $(D_{ii})_0$ is found to be dominated by the product of μ_{ii} and the corresponding main-term ODC $(L_{ii})_0$.

In multicomponent systems, each cross-term diffusion coefficient $(D_{ij})_0$ ($i \neq j$) links the gradient of one component to the flux of another and can be written as a sum involving main- and cross-term ODCs. For $(D_{21})_0$ in our ternary systems, we will see that the contribution of $(L_{21})_0 \mu_{11}$ is very small compared to that of $(L_{22})_0 \mu_{21}$. In contrast, for $(D_{12})_0$, the contributions of $(L_{12})_0 \mu_{22}$ and $(L_{11})_0 \mu_{12}$ are similar in magnitude but opposite in sign.

Materials and Methods

The Gosting diffusimeter and its modifications, other apparatus, solution preparation, pH adjustment, temperature

TABLE 1: Ternary Diffusion Data for 0.6 mM Lysozyme Chloride–KCl–H₂O at pH 4.5 and 25 °C

	$C_2 = 0.25$ M	$C_2 = 0.50$ M	$C_2 = 0.90$ M	$C_2 = 1.20$ M	$C_2 = 1.50$ M
$(D_{11})_V$ (10^{-9} m ² s ⁻¹)	0.1281 ± 0.0001	0.1237 ± 0.0001	0.1203 ± 0.0001	0.1181 ± 0.0001	0.1155 ± 0.0001
$(D_{12})_V$ (10^{-9} m ² s ⁻¹)	0.000044 ± 0.000002	0.000049 ± 0.000001	0.000056 ± 0.000002	0.000058 ± 0.000002	0.000062 ± 0.000002
$(D_{21})_V$ (10^{-9} m ² s ⁻¹)	11.8 ± 0.3	16.9 ± 0.2	26.1 ± 0.3	33.4 ± 0.1	41.9 ± 0.1
$(D_{22})_V$ (10^{-9} m ² s ⁻¹)	1.817 ± 0.001	1.829 ± 0.001	1.863 ± 0.001	1.891 ± 0.001	1.922 ± 0.001
d (g cm ⁻³)	1.01122 ₇	1.02275 ₆	1.04080 ₃	1.05417 ₆	1.06745 ₀
\bar{V}_1 (cm ³ mol ⁻¹)	10191	10138	10258	10224	10190
\bar{V}_2 (cm ³ mol ⁻¹)	28.549	28.916	29.701	30.303	30.610
\bar{V}_0 (cm ³ mol ⁻¹)	18.065	18.062	18.052	18.041	18.033
$(D_{11})_0$ (10^{-9} m ² s ⁻¹)	0.1291	0.1248	0.1216	0.1195	0.1171
$(D_{12})_0$ (10^{-9} m ² s ⁻¹)	0.00007581	0.00008170	0.00009068	0.00009427	0.00009963
$(D_{21})_0$ (10^{-9} m ² s ⁻¹)	12.22	17.79	27.97	36.18	45.79
$(D_{22})_0$ (10^{-9} m ² s ⁻¹)	1.830	1.856	1.915	1.964	2.016

control at 25 °C, methods of measurement, and data reduction procedures were described in our previous papers.^{6–8} Solutions were prepared from Mallinckrodt 99.9% analytical reagent grade KCl dried at 400 °C overnight and from Seikagaku-lyophilized 6× recrystallized lysozyme (lot #E96Y03). As in our earlier work, lysozyme chloride was manipulated in a drybox, and solutions with volumes of 50–70 mL were prepared by weight (corrected to mass) with ±0.1 mg precision, based on molecular masses of $M_1 = 14\,307$ g mol⁻¹ for lysozyme,¹⁹ $M_2 = 74.551$ g mol⁻¹ for KCl, and 18.015 g mol⁻¹ for H₂O. A Corning 135 pH meter with an Orion 8102 ROSS combination pH electrode, standardized with Corning reference solutions, was used to measure the pH both for solutions used for diffusion measurements and for determining the protein charge by titration methods.²⁰ Experimental details on the determination of ternary diffusion coefficients are available as Supporting Information.

Results and Discussion

Ternary Diffusion Results. Table 1 lists the volume-fixed $(D_{ij})_V$ values calculated^{18,21,22} with data from all four experiments at each of the five mean KCl concentrations (see Supporting Information). This table also includes the density d and the partial molar volumes \bar{V}_1 , \bar{V}_2 , and \bar{V}_0 obtained from volumetric measurements and the $(D_{ij})_0$ values for the solvent-fixed reference frame, calculated from the volume-fixed $(D_{ij})_V$ and \bar{V}_i using eq 2 in ref 16.

Figure 1 show the $(D_{ij})_V$ as functions of C_2 at constant C_1 for all three salts. Figure 1d also shows the binary diffusion coefficient D_V for each salt.

Extraction of Thermodynamic Properties. Here, we show how several thermodynamic properties of these ternary solutions can be extracted from the measured diffusion coefficients, in some cases with considerably greater precision than obtainable

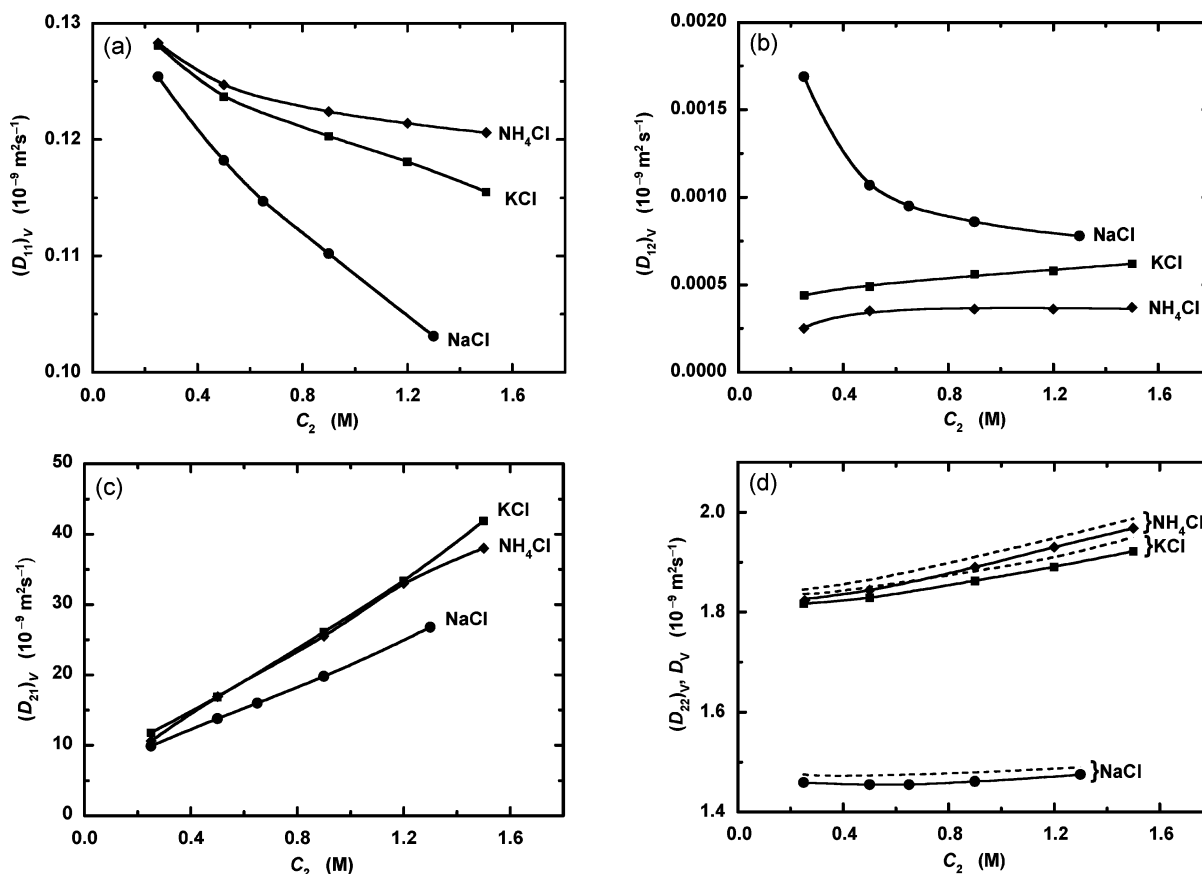


Figure 1. Volume-fixed diffusion coefficients for the ternary system lysozyme chloride + MCl + H₂O as a function of MCl concentration, C_2 , at $C_1 = 0.6$ mM, pH 4.5, and 25 °C: (a) $(D_{11})_V$, (b) $(D_{12})_V$, (c) $(D_{21})_V$, (d) $(D_{22})_V$ and D_V ; ●, M = Na; ■, M = K; ◆, M = NH₄. The solid curves are smoothed through the ternary experimental points, and the dashed curves are smoothed through the omitted binary diffusion coefficients, D_V , from the literature.^{57–59}

TABLE 2: Chemical Potential Derivatives for 0.6 mM Lysozyme Chloride–KCl–H₂O at pH 4.5 and 25 °C

	$C_2 = 0.25$ M	$C_2 = 0.50$ M	$C_2 = 0.90$ M	$C_2 = 1.20$ M	$C_2 = 1.50$ M
μ_{11}/RT (M ⁻¹)	1918	1793	1737	1720	1709
μ_{22}/RT (M ⁻¹)	7.130	3.598	2.052	1.579	1.300
μ_{12}/RT (M ⁻¹)	31.5	17.4	11.9	10.5	10.5
μ_{21}/RT (M ⁻¹)	49.7	35.6	30.6	29.7	30.0

by other approaches. The extracted data provide the basis for a firm thermodynamic understanding of diffusion and crystallization in ternary aqueous solutions of lysozyme chloride and a 1:1 chloride salt, corresponding to our first main objective.

Chemical Potential Derivatives. The thermodynamic derivatives $\mu_{12} = \partial\mu_1/\partial C_2$ and $\mu_{21} = \partial\mu_2/\partial C_1$ for ternary solutions are extracted from diffusion data using

$$\mu_{12} = \frac{\mu_{11}[C_1\bar{V}_2(D_{22})_0 - (1 - C_1\bar{V}_1)(D_{12})_0] - \mu_{22}[C_2\bar{V}_1(D_{22})_0 - (1 - C_1\bar{V}_1)(D_{21})_0]}{(1 - C_2\bar{V}_2)(D_{22})_0 - (1 - C_1\bar{V}_1)(D_{11})_0} \quad (5a)$$

$$\mu_{21} = \frac{\mu_{11}[C_1\bar{V}_2(D_{11})_0 - (1 - C_2\bar{V}_2)(D_{12})_0] - \mu_{22}[C_2\bar{V}_1(D_{11})_0 - (1 - C_2\bar{V}_2)(D_{21})_0]}{(1 - C_2\bar{V}_2)(D_{22})_0 - (1 - C_1\bar{V}_1)(D_{11})_0} \quad (5b)$$

which are obtained from the ORR and the cross-derivative relation $(\partial\mu_1/\partial m_2)_{T,p,m_1} = (\partial\mu_2/\partial m_1)_{T,p,m_2}$,⁷ where m_i is the molality of component i . We make extensive use of the derivative expressions for the μ_{ij} ,²³ which for a ternary solution of z_p :1 and 1:1 electrolytes having a common anion are

$$\begin{bmatrix} \mu_{11} & \mu_{12} \\ \mu_{21} & \mu_{22} \end{bmatrix} = RT \begin{bmatrix} \frac{1}{C_1} + \frac{z_p^2}{z_p C_1 + C_2} + (z_p + 1) \frac{\partial \ln y_1}{\partial C_1} & \frac{z_p}{z_p C_1 + C_2} + (z_p + 1) \frac{\partial \ln y_1}{\partial C_2} \\ \frac{z_p}{z_p C_1 + C_2} + 2 \frac{\partial \ln y_2}{\partial C_1} & \frac{1}{C_2} + \frac{1}{z_p C_1 + C_2} + 2 \frac{\partial \ln y_2}{\partial C_2} \end{bmatrix} \quad (6)$$

where z_p is both the effective charge on the lysozyme cation and the effective stoichiometric coefficient of chloride in lysozyme chloride and y_1 and y_2 are the molar mean ionic activity coefficients of the lysozyme chloride and salt components, respectively.⁷

Successful use of these equations depends on appropriately good estimates of μ_{11} and μ_{22} , as discussed below. In turn, these are possible in the “asymmetric” case of small C_1 and C_2 large compared to C_1 , which occurs in many systems of biochemical interest.⁷

For the ternary protein solutions with 1:1 salts that we have studied, terms involving μ_{11} contribute only 1–2% to the calculated values of μ_{12} and μ_{21} in eq 5a and eq 5b. Furthermore, estimates^{24,25} of the second virial coefficient show that the activity coefficient term in the expression for μ_{11} in eq 6 does not exceed 20% of μ_{11} . Therefore, negligible error in μ_{12} and μ_{21} (<0.4%) will result from approximating μ_{11} by its first two terms in eq 6.

Estimates of μ_{22} in this system are based on the expectation that while μ_2 should depend on protein concentration, its derivative μ_{22} should be close to $(\partial\mu_{\text{salt}}/\partial C_{\text{salt}})_{T,p}$ for the binary salt case because of the low concentration of protein relative to the salt. Furthermore, the data show that $(D_{22})_V$ for diffusion of each salt due to its own concentration gradient is just 1–2% lower than the diffusion coefficient in its aqueous binary

solution, D_V , at the corresponding salt concentration (see Figure 1d). Since diffusion is driven by chemical potential gradients, the near equality of $(D_{22})_V$ and D_V for the salt component in the ternary and binary systems is strong evidence that taking $\mu_{22} = (\partial\mu_{\text{salt}}/\partial C_{\text{salt}})_{T,p}$ is an excellent approximation.

Since protein–salt thermodynamic interactions are described by the cross-chemical potential derivatives based on molality: $\mu_{12}^{(m)} \equiv (\partial\mu_1/\partial m_2)_{T,p,m_1} = (\partial\mu_2/\partial m_1)_{T,p,m_2}$,²⁶ we report their relationship with the μ_{ij} ²³

$$\mu_{12}^{(m)} = \frac{1000d - C_1 M_1 - C_2 M_2}{1000} (\mu_{21}(1 - C_1\bar{V}_1) - \mu_{22}C_2\bar{V}_1) \quad (7)$$

Our use of multicomponent diffusion coefficients to extract thermodynamic properties allows us to accurately determine the dependence of μ_{12} and μ_{21} on salt concentration C_2 and to examine common-ion and nonideality effects.²⁷

The quantities μ_{11} and μ_{22} are estimated following the procedure described in ref 7 and summarized above. Activity coefficient derivatives for binary aqueous KCl at 25 °C were taken from ref 28. In Table 2, we show the estimated values of $\mu_{11}/(RT)$ and $\mu_{22}/(RT)$ and extracted values of $\mu_{12}/(RT)$ and $\mu_{21}/(RT)$. The latter two values are also shown in Figure 2, which include, for comparison, our reported values of $\mu_{12}/(RT)$ and $\mu_{21}/(RT)$ for $C_1 = 0.6$ mM at pH 4.5 and 25 °C for lysozyme chloride ($C_1 = 0.6$ mM) in aqueous NaCl⁶ and NH₄Cl⁷ at several salt concentrations.

Figure 2 shows that μ_{12} and μ_{21} are positive and decrease as salt concentration increases. This is easily understood from eq 6, in which $z_p/(z_p C_1 + C_2)$ is a dominant term that varies approximately as z_p/C_2 . This contribution is related to the polyelectrolyte nature of the electrically neutral protein component, consisting of a lysozyme cation and z_p chloride counterions. However, chloride is also the common anion of the added salt, and the chloride concentration depends strongly on C_2 . In eq 6, we see that the other terms are related to nonideality. The precision of our μ_{12} and μ_{21} values allows us to estimate the effective protein charge z_p and to distinguish and quantify the common-ion and nonideality contributions.

Protein Charge. We can regress the expressions of μ_{12} and μ_{21} in eq 6 to estimate z_p in aqueous solutions of lysozyme in KCl, as shown earlier for NaCl⁷ and NH₄Cl.⁸ We expand both activity coefficient derivatives as polynomials in solution normality $z_p C_1 + C_2$ for each salt over its experimental concentration range. Retaining only linear terms yields

$$(z_p + 1)(\partial \ln y_1/\partial C_2) = a_{12} + b_{12}(z_p C_1 + C_2) \quad (8a)$$

$$2(\partial \ln y_2/\partial C_1) = a_{21} + b_{21}(z_p C_1 + C_2) \quad (8b)$$

To determine the number of fitting parameters sufficient for regression, we first retained only a_{12} and a_{21} in eqs 8a and 8b, respectively, and then included the higher-order parameters b_{12} and b_{21} for comparison. For KCl, this inclusion led to a significantly improved regression of eqs 8a and 8b and, consequently, better accuracy of z_p , as previously found for NaCl⁷ but not for NH₄Cl.⁸ For KCl, the experimental error is somewhat higher than that for the other two salts, and retaining

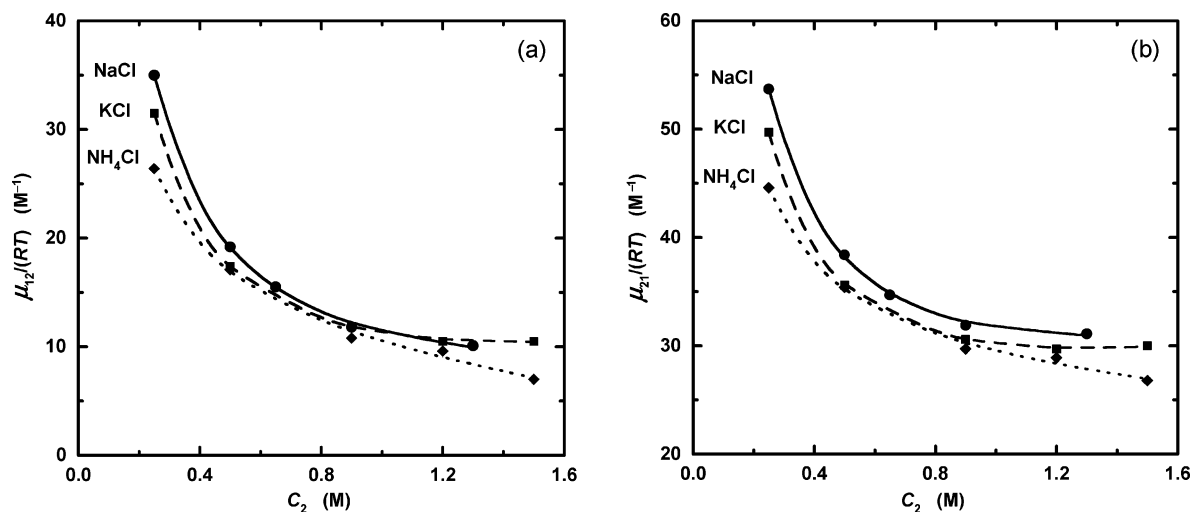


Figure 2. Cross derivatives of the chemical potential as a function of MCl concentration, C_2 , at pH 4.5 and 25 °C: (a) $\mu_{12}/(RT)$, (b) $\mu_{21}/(RT)$; ●, M = Na; ■, M = K; ◆, M = NH_4 . The curves (—, M = Na; ---, M = K; ···, M = NH_4) are fitted to the data using eqs 7a and 7b. The fitting parameters are given in Table 3.

TABLE 3: Parameters from Fits of $\mu_{12}/(RT)$ and $\mu_{21}/(RT)$ versus Salt Concentration

Parameters for $\mu_{12}/(RT)$				
salt	z_p	$a_{12} (\text{M}^{-1})$	$b_{12} (\text{M}^{-2})$	RMSE ^a
NaCl	8.5 ± 0.3	1.5 ± 1.2	1.5 ± 0.9	0.35
NH_4Cl	5.7 ± 0.4	4.4 ± 0.9		1.12
KCl	7.7 ± 0.2	0.5 ± 0.6	3.2 ± 0.4	0.17
Parameters for $\mu_{21}/(RT)$				
salt	z_p	$a_{21} (\text{M}^{-1})$	$b_{21} (\text{M}^{-2})$	RMSE ^a
NaCl	8.6 ± 0.3	18.9 ± 1.2	4.2 ± 0.9	0.34
NH_4Cl	5.3 ± 0.3	24.0 ± 0.6		0.74
KCl	7.9 ± 0.1	17.6 ± 0.3	4.7 ± 0.2	0.10

^a Denotes root-mean-square error.

only a_{12} and a_{21} in eqs 8a and 8b gave satisfactory estimates of z_p . Values of z_p , a_{12} , a_{21} , b_{12} , and b_{21} obtained by regression for the NaCl and NH_4Cl cases^{7,8} are included in Table 3 with those for KCl. Uncertainties of the coefficients are also reported, as well as the root-mean-square error of each regression. Agreement between z_p values calculated from μ_{12} and μ_{21} is a test of our data and assumptions and is very good for each salt.

The z_p values calculated using eqs 8a and 8b correspond to the protein cation's "effective charge" and are lower than the "net titration charge".²⁹ This is expected, since the latter is based only on the degree of protonation and does not account for counterion binding. For all three salts at pH 4.5, our titrations³⁰ showed that this net charge ranges from 10.8 to 11.2 at $C_2 = 0.25$ and 0.9 M, in agreement with the results of Tanford and Wagner.²⁰ By comparison, the calculated effective charges are approximately 8.6, 5.5, and 7.8 for NaCl, NH_4Cl , and KCl, respectively.

Impact of Common-Ion Effect. It is usually assumed that the common-ion effect is significant only at low salt concentrations.³¹ Consequently, at higher salt concentrations, the increase of protein chemical potential with salt concentration is usually described only in terms of deviation from ideality, i.e., by preferential exclusion of salt from the protein surface (by preferential hydration). However, a_{12} and b_{12} values for all three salts in Table 3, together with eq 6, show that the common-ion contribution to the derivative μ_{12} is still dominant at $C_2 = 0.25$ M. At the highest salt concentration, this contribution is reduced to about 50% of the total.

TABLE 4: Chemical Potential Derivatives, $\mu_{12}^{(m)}/RT$ for 0.6 mM Lysozyme Chloride in the Presence of NaCl, KCl, and NH_4Cl – H_2O at pH 4.5 and 25 °C^a

C_2 (M)	$\mu_{12}^{(m)}/RT$ (NaCl)	$\mu_{12}^{(m)}/RT$ (KCl)	$\mu_{12}^{(m)}/RT$ (NH_4Cl)
0.25	34.3	30.7	25.6
0.5	18.7	16.7	16.3
0.65	14.9	(13.6)	(12.4)
0.9	11.3	11.1	9.9
1.2	(9.8)	9.7	8.7
1.3	9.5	(9.6)	(7.4)
1.5	(9.0)	9.4	6.1

^a The values in parentheses are obtained by interpolation.

Thus, for lysozyme chloride, our results clearly show that the common-ion effect is still very important at the higher salt concentrations relevant to crystallization and, therefore, plays a significant role in determining both the dependence of protein solubility on salt concentration and the effectiveness of the salt as a precipitant. Reaillieu et al.³² have shown the importance of the protein net charge and long-range electrostatic interactions for protein solubility. Furthermore, studies from the group of Ducruix^{33–35} and Tardieu^{36,37} have demonstrated that lysozyme solubility is significantly affected by the nature of salt anions (i.e., the common ion). Our results are consistent with their findings and represent a new important contribution to previous work. This point will be further discussed in relation to protein solubility (see Thermodynamic and Crystal Growth Applications).

Protein-Salt Thermodynamic Interactions. We now address our second objective. In Table 4, we report the values of $\mu_{12}^{(m)}/RT$ obtained using eq 7.³⁸ We observe that they are approximately equal to the corresponding values of μ_{12}/RT as expected. The cross-derivative $\mu_{12}^{(m)}$ (or μ_{12}) describes the effect of a given salt in changing the lysozyme chemical potential and thus represents the protein–salt thermodynamic interaction in solution.²⁶ Our positive values of $\mu_{12}^{(m)}$ can be used to rank the three salts with respect to their effectiveness in increasing the lysozyme chemical potential and thus favoring protein precipitation. Examination of Table 4 (for $\mu_{12}^{(m)}/RT$) and Figure 2a (for μ_{12}/RT) shows that the corresponding values increase in the sequence $\text{NH}_4\text{Cl} < \text{KCl} < \text{NaCl}$ for a given salt concentration with $C_2 < 0.9$ M. For $C_2 \geq 0.9$ M, the values of $\mu_{12}/(RT)$ for KCl and NaCl become approximately equal, while the corresponding values for NH_4Cl remain somewhat lower (see Figure

TABLE 5: Onsager Transport Coefficients for Given KCl Concentrations (C_2) for 0.6 mM Lysozyme Chloride–KCl–H₂O at pH 4.5 and 25 °C

	$C_2 = 0.25$ M	$C_2 = 0.50$ M	$C_2 = 0.90$ M	$C_2 = 1.20$ M	$C_2 = 1.50$ M
$RTL_{11}/(z_p C_1)$ (10^{-9} m ² s ⁻¹)	0.01577	0.01593	0.01605	0.01611	0.01631
$RTL_{12}/(z_p C_1)$ (10^{-9} m ² s ⁻¹)	-0.068	-0.072	-0.084	-0.095	-0.116
$RTL_{22}/(z_p C_2)$ (10^{-9} m ² s ⁻¹)	1.033	1.035	1.039	1.039	1.037

2a). We also observe that since $\mu_1(C_2)$ for the three salts must approach the same common value $\mu_1(0)$ as $C_2 \rightarrow 0$, our results imply that $\mu_1(C_2) = \mu_1(0) + \int_0^{C_2} \mu_{12}(C_2) dC_2$ also increases in the sequence $\text{NH}_4\text{Cl} < \text{KCl} < \text{NaCl}$ at any given concentration within the experimental domain. This ranking of the three salts is consistent with the order of the Hofmeister solubility series.

Interpretation of Ternary Diffusion Coefficients. In this section, we analyze and interpret the dependence of the four ternary diffusion coefficients on salt concentration, corresponding to our third main objective. The analysis is partly qualitative and partly quantitative. It provides new insight into charge and common-ion effects, into the cross-terms characterizing coupled transport in aqueous solutions of globular proteins, and more generally into the transport of other macromolecules.

We restate the important fact that our systems are “asymmetric”, in the sense that the molar concentration of salt is much larger than that of the protein. We will consider the protein–salt transport properties in light of this asymmetry.

Modeling Considerations. We first discuss the Stokes–Einstein approximation to the effect of viscosity on the diffusion coefficient of Brownian particles and then consider the ternary Nernst–Hartley equations, both of which we use to interpret the measured multicomponent diffusion coefficients.

At infinite dilution, diffusion coefficients of Brownian particles in a continuum fluid are frequently approximated using the Stokes–Einstein equation²⁹ $D = k_B T / (6\pi r_H^{\text{eq}} \eta)$, where k_B is the Boltzmann constant, r_H^{eq} is the equivalent hydrodynamic radius, and η is the viscosity of the continuum fluid, which in this case is the interstitial aqueous salt solution. The prediction that the macromolecular diffusion coefficient, which is small compared to that of the small ions, will decrease as one increases the viscosity of the surrounding continuum of solvent and small ions, is borne out even at nonzero concentrations of the macromolecular component.

We now consider the electrolyte nature of the system. The four diffusion coefficients of the solutes depend in part on the mobilities of the constituent ions, constrained by the requirement of electroneutrality. The Nernst–Hartley (N-H) equations for electrolyte systems describe this coupled transport of ions only at infinite dilution and do not account for thermodynamic nonideality and Onsager–Fuoss electrophoretic effects.³⁹ Gosting⁴⁰ discussed application of the N-H equations to protein solutions.

For our ternary electrolyte system, the N-H equations are

$$\begin{bmatrix} D_{11} & D_{12} \\ D_{21} & D_{22} \end{bmatrix} = \begin{bmatrix} \tilde{D}_p \left[1 + \frac{z_p^2 \tilde{C}_p}{\Delta} (\tilde{D}_{\text{Cl}} - \tilde{D}_p) \right] & \tilde{D}_p \frac{z_p \tilde{C}_p}{\Delta} (\tilde{D}_{\text{Cl}} - \tilde{D}_M) \\ \tilde{D}_M \frac{z_p \tilde{C}_M}{\Delta} (\tilde{D}_{\text{Cl}} - \tilde{D}_p) & \tilde{D}_M \left[1 + \frac{\tilde{C}_M}{\Delta} (\tilde{D}_{\text{Cl}} - \tilde{D}_M) \right] \end{bmatrix} \quad (9)$$

where our denominator $\Delta = z_p^2 \tilde{C}_p \tilde{D}_p + \tilde{C}_M \tilde{D}_M + \tilde{C}_{\text{Cl}} \tilde{D}_{\text{Cl}}$ is equivalent to that of Gosting,⁴⁰ whose equations are written in terms of electroneutral components. Since the N-H equations pertain only at infinite dilution, where the solvent- and volume-

fixed frames coincide, the D_{ij} require no reference-frame subscripts. In eq 9, \tilde{D}_p , \tilde{D}_M , and \tilde{D}_{Cl} are the infinite dilution tracer diffusion coefficients of the protein cation, salt co-ion (Na^+ , NH_4^+ , or K^+), and chloride ion (the common ion), respectively, and \tilde{C}_p , \tilde{C}_M , and \tilde{C}_{Cl} are the corresponding concentrations. The value of \tilde{D}_p for the lysozyme cation in water at pH 4.5, determined using the Gosting diffusimeter, is 0.132×10^{-9} m² s⁻¹.³⁰

The tracer diffusion coefficients for small ions have been calculated⁴¹ from limiting ionic mobilities³⁹ and thus pertain to infinitely dilute aqueous solutions. For Na^+ , NH_4^+ , K^+ , and Cl^- , they are 1.33, 1.96, 1.96, and 2.03×10^{-9} m² s⁻¹, respectively. For our systems, we have $z_p^2 \tilde{C}_p \tilde{D}_p \ll C_2 (\tilde{D}_M + \tilde{D}_{\text{Cl}})$ (consistent with $z_p \tilde{C}_1 \ll C_2$), so that to good approximation in very dilute solutions, the N-H equations in our case become

$$\begin{bmatrix} D_{11} & D_{12} \\ D_{21} & D_{22} \end{bmatrix} = \begin{bmatrix} \tilde{D}_p \left[1 + \frac{z_p^2 C_1}{C_2} \frac{(\tilde{D}_{\text{Cl}} - \tilde{D}_p)}{\tilde{D}_M + \tilde{D}_{\text{Cl}}} \right] & \tilde{D}_p \frac{z_p C_1}{C_2} \frac{\tilde{D}_{\text{Cl}} - \tilde{D}_M}{\tilde{D}_M + \tilde{D}_{\text{Cl}}} \\ \frac{z_p}{\tilde{D}_M + \tilde{D}_{\text{Cl}}} \frac{\tilde{D}_M (\tilde{D}_{\text{Cl}} - \tilde{D}_p)}{\tilde{D}_M + \tilde{D}_{\text{Cl}}} & \frac{2 \tilde{D}_M \tilde{D}_{\text{Cl}}}{\tilde{D}_M + \tilde{D}_{\text{Cl}}} \end{bmatrix} \quad (10)$$

where we have used \tilde{C}_p and C_1 and $\tilde{C}_M = \tilde{C}_{\text{Cl}} C_2$.

From eq 10, we see that D_{11} is larger than the infinite-dilution tracer diffusion coefficient of the protein cation, \tilde{D}_p .

A gradient of component 1 gives gradients of lysozyme cations and chloride anions. To preserve electroneutrality, the faster chloride counterions will electrostatically drag the slower lysozyme cations, thereby generating a flux of lysozyme chloride, corresponding to $D_{11} > \tilde{D}_p$. However, as the concentration of salt (component 2) increases, the counterions will drag lysozyme cations and co-ions according to their relative concentrations and charges. As \tilde{C}_2 continues to increase, i.e., as $z_p C_1 / C_2$ decreases, chloride ions will overwhelmingly drag co-ions, so that in the limit lysozyme will diffuse following its intrinsic mobility \tilde{D}_p .

In eq 10, we have assumed that the salt is present in relatively large excess with respect to the protein. Consequently, as expected, the N-H expression for \tilde{D}_{22} is the same as that for the diffusion coefficient in the corresponding binary salt solution.

Onsager Diffusion Coefficients. The transport coefficients (L_{ij})₀, also called “diffusion Onsager coefficients”, are in the solvent-fixed frame of reference and can be calculated after inverting eqs 4a–d (see eq 7 in ref 7). Our results are reported in Table 5. We observe that the accuracy of the three ODCs (L_{11})₀ and (L_{12})₀ = (L_{21})₀ is directly related to the accuracy of μ_{11} . The (L_{ij})₀ μ_{ijk} contributions to the experimental diffusion coefficients can be estimated from eqs 4a–d. We call the comparison of the sizes of these contributions the “ODC analysis”; it will be used for the interpretation of the cross-diffusion coefficients.

Examination of (D_{11})_v. Values of (D_{11})_v for aqueous lysozyme chloride at 0.6 mM and various concentrations of MCl (M = Na, NH₄, or K) at pH 4.5 are shown in Figure 1a. In each case,

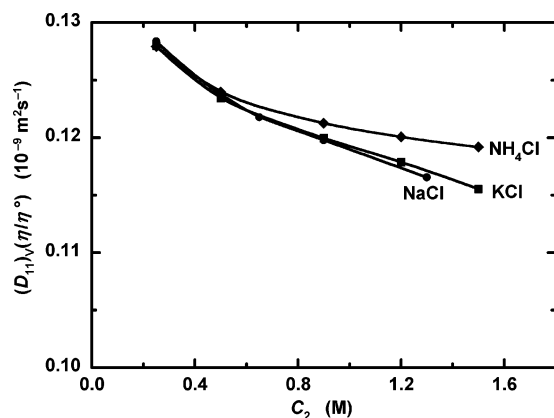


Figure 3. The product $(D_{11})_v\eta/\eta_0$ as a function of MCl concentration, C_2 , at pH 4.5 and 25 °C: ●, M = Na; ■, M = K; ◆, M = NH_4 . The curves are smoothed through the data.

the diffusion coefficient $(D_{11})_v$ decreases as salt concentration increases. The decrease is larger for lysozyme chloride in aqueous NaCl than in aqueous KCl and, in turn, is larger in aqueous KCl than in aqueous NH_4Cl .

The decrease of $(D_{11})_v$ with C_2 can be ascribed to at least two factors. One is the electrostatic coupling between the macroion and the common anion, predicted by N-H as discussed above. A second important factor is the increase of solution viscosity with increasing C_2 (according to the Stokes–Einstein equation). To evaluate this effect, we multiply the $(D_{11})_v$ values by η/η_0 , the relative viscosity of each binary saltwater system,^{42,43} where η is the viscosity of the interstitial binary salt solution, and η_0 is the viscosity of water. Comparing Figures 1a and 3 shows that over the range of C_2 , $(D_{11})_v\eta/\eta_0$ varies considerably less for KCl than does the measured $(D_{11})_v$. Figure 3 also shows that $(D_{11})_v\eta/\eta_0$ values for NaCl and KCl are nearly identical over the entire range of C_2 , strongly suggesting that the increasing divergence between the $(D_{11})_v$ values as the concentrations of these two salts increase is due almost entirely to viscous effects (plots of $(D_{11})_0\eta/\eta_0$ for each salt are nearly identical to those shown in Figure 3). These results suggest that as C_2 increases, effects other than viscosity contribute significantly to divergence between measured values of $(D_{11})_v$ in aqueous NH_4Cl on one hand and in aqueous NaCl or KCl on the other. Possible contributors are more specific short-range protein–salt interactions affecting both thermodynamic factors and protein mobilities.

Examination of $(D_{22})_v$. Values of ternary $(D_{22})_v$ versus C_2 are shown in Figure 1d for aqueous lysozyme chloride solutions with NaCl, NH_4Cl , and KCl, along with values of D_v for the corresponding binary systems. We find that $(D_{22})_v$ is only 1–2% less than the corresponding D_v . This is not surprising, because in our ternary systems the salt behaves essentially as it does in the corresponding binary system. This small difference is consistent with an expected small obstruction effect of the protein macromolecules on the motion of the small salt ions.

Examination of $(D_{12})_v$. For each salt at each concentration, values of $(D_{12})_v$ shown in Figure 1b are much smaller than the other three diffusion coefficients. Both the magnitude of $(D_{12})_v$ and its dependence on salt concentration differ among the three salts. We find that at low salt concentrations, the values of $(D_{12})_v$ follow the decreasing order $\text{NaCl} \gg \text{KCl} > \text{NH}_4\text{Cl}$. The difference between $(D_{12})_v$ for NaCl and KCl is dramatically reduced as salt concentration increases, with $(D_{12})_v$ being somewhat lower for NH_4Cl . As C_2 increases, Figure 1b shows that $(D_{12})_v$ decreases for NaCl and increases for KCl and NH_4Cl . Since $(D_{12})_v$ is the only diffusion coefficient for which

the behavior is so qualitatively different among the three salts, understanding these experimentally observed differences is of interest.

Some features of the dependence of $(D_{12})_v$ on the nature and concentration of the salt can be qualitatively understood on the basis of N-H considerations. The approximate N-H equation, eq 10, shows that the magnitude of $(D_{12})_v$ is inversely proportional to C_2 , qualitatively consistent with the experimental behavior in aqueous NaCl, and is directly proportional to the difference $\tilde{D}_{\text{Cl}} - \tilde{D}_{\text{M}}$, which is $0.70 \times 10^{-9} \text{ m}^2 \text{ s}^{-1}$ for NaCl, versus $0.07 \times 10^{-9} \text{ m}^2 \text{ s}^{-1}$ for KCl and NH_4Cl .

For KCl and NH_4Cl , \tilde{D}_{Cl} and \tilde{D}_{M} are very close. Thus, the Coulombic mechanism, accounted for by the infinite-dilution N-H equations, does not provide even a qualitatively correct estimate of either $(D_{12})_v$ at low concentrations or the C_2 dependence of $(D_{12})_v$. This suggests that when the magnitude of $\tilde{D}_{\text{Cl}} - \tilde{D}_{\text{M}}$ is small, other factors not accounted for by the N-H equations determine the dependence of $(D_{12})_v$ on C_2 at any nonzero C_1 .

To understand the observed concentration dependence of $(D_{12})_v$, we need a more general description than the N-H equations, which are strictly valid only in the limit of infinite dilution. We thus proceed with an ODC analysis. We note that $(L_{11})_0\mu_{12} \approx -(L_{12})_0\mu_{22}$, so that, considering eq 4b, $(D_{12})_0$, and thus $(D_{12})_v$, is a small difference between two larger contributions. Therefore, an attempt to understand the behavior of $(D_{12})_0$ using only eq 4b would seem unfeasible. Nonetheless, we find that if eq 4b is rearranged in the form of a product, we can interpret the behavior of $(D_{12})_0$. We write eq 4b as

$$(D_{12})_0 = (L_{11})_0\mu_{12}\{1 + [(L_{12})_0/(L_{11})_0]\mu_{22}/\mu_{12}\} = (L_{11})_0\mu_{12}W \quad (11)$$

The factor $(L_{11})_0$, directly related to the transport of the protein, is approximately constant as C_2 is increased at constant C_1 (see Table 4). Moreover, the $(L_{11})_0$ value^{7,8} is not sensibly affected by the nature of the salt. These observations allow us to relate the relevant variation of $(D_{12})_0$ to only μ_{12} and the factor W defined by the second equality in eq 10.

Equation 11 permits us to focus, using the μ_{12} and W factors, on the very different low-concentration behavior of $(D_{12})_0$ for the NaCl case in comparison to the KCl and NH_4Cl cases.

In the previous subsection, we found that μ_{12} decreases significantly with C_2 for all three salts and attributed the decreases to the contribution of the common-ion term in eq 6. Because the μ_{12} (Figure 2a) and $(D_{12})_0$ (Figure 1b) values have different qualitative behaviors for the three salt systems, μ_{12} cannot account for the significant differences between the NaCl case and the KCl and NH_4Cl cases.

The quantity W can be obtained from eq 10, where $(L_{11})_0$ and $(L_{12})_0$ are taken from Table 5. Note that since $(L_{12})_0/(L_{11})_0$ depends only very weakly on μ_{11} , the accuracy of this ratio is improved compared to $(L_{12})_0$ alone. At low salt concentrations, W is a measure of the electrostatic coupling between the protein and the salt. In the limit, where $C_2 \rightarrow 0$ and $C_1/C_2 \rightarrow 0$, we can use eq 28 of ref 44 with the limiting values to obtain

$$W_{\text{lim}} = \frac{\tilde{D}_{\text{Cl}} - \tilde{D}_{\text{M}}}{\tilde{D}_{\text{Cl}} + \tilde{D}_{\text{M}}} \quad (12)$$

Equation 12 shows that W will reach a finite limit as $C_2 \rightarrow 0$, which suggests that W can be expanded in a power series in C_2 . Using eq 11, we find that W increases with salt concentration for each salt and can be closely approximated by a linear function $W(C_2) = W(0) + (dW/dC_2)C_2$. We find that the slopes

for the three salts are approximately equal. The intercept, $W(0)$, is about 0.05 for NaCl, and virtually zero for KCl and NH_4Cl as expected from eq 12 because $\tilde{D}_{\text{Cl}} \approx \tilde{D}_{\text{M}}$. This is the main factor distinguishing the $(D_{12})_0$ behavior for NaCl from that for KCl and NH_4Cl .

To examine the dependence of $(D_{12})_0$ on C_2 , we approximate eq 11 by

$$(D_{12})_0 \approx (L_{11})_0 [z_p/C_2 + a_{12} + b_{12}C_2] [W(0) + (dW/dC_2)C_2] \quad (13)$$

where the coefficients a_{12} and b_{12} (describing the activity coefficient derivative for μ_{12}) are shown in Table 3, and we have neglected $z_p C_1$ in the second factor. From eq 13, we see that if $W(0)$ is significant, then the $(L_{11})_0 W(0) z_p / C_2$ term, which is inversely proportional to C_2 , will be significant. This is the case for NaCl. However, if $W(0)$ is negligible, then $(D_{12})_0$ will increase with increasing salt concentration. This increase is related to the positive nonideal term of μ_{12} . The numerical differences in the dependence of $(D_{12})_0$ on salt concentration between NH_4Cl and KCl appear to be due to the differences in the C_2 dependence of μ_{12} .

Examination of $(D_{21})_V$. Values of $(D_{21})_V$ for NaCl, NH_4Cl , and KCl at pH 4.5 are shown in Figure 1c. These are the largest of the four diffusion coefficients at each salt concentration. For each salt, $(D_{21})_V$ increases roughly linearly with C_2 at $C_1 = 0.6$ mM and is considerably larger than both main terms. At higher salt concentrations, $(D_{21})_V$ is more than 10 times the main-term coefficient $(D_{22})_V$ and approximately 100 to 350 times $(D_{11})_V$. Thus, when the three salt systems have a uniform salt concentration but have a gradient of protein concentration, roughly 100 mol of salt will be transported with each mole of protein at the lower end of our C_2 range and up to 350 mol per mole of protein at the higher end. Among other effects, this will lead to an increase in salt transport to the interface of a growing crystal, where the higher salt concentration can lead to increased inclusion of salt in the crystal. We note that the pseudo-binary approximation cannot predict or interpret such results.

The experimental plots of $(D_{21})_0/(D_{22})_0$ vs C_2 for the three salts are nearly linear and parallel (see Figure 4). A thermodynamic explanation of this behavior follows.

An ODC analysis shows that in all cases $(D_{21})_0$ is dominated by $(L_{22})_0 \mu_{21}$, with the $(L_{21})_0 \mu_{11}$ term being negative and about 2–5% of the total. Similarly, $(D_{22})_0$ is dominated by $(L_{22})_0 \mu_{22}$. Therefore, we can closely approximate $(D_{21})_0/(D_{22})_0$ by μ_{21}/μ_{22} . Tables 1 and 2 support this, since the calculated ratios of $(D_{21})_0/(D_{22})_0$ to μ_{21}/μ_{22} are 0.97 ± 0.01 . Furthermore, Table 1 shows that $[(D_{21})_V/(D_{22})_V]/[(D_{21})_0/(D_{22})_0] = 0.956 \pm 0.02$. Therefore, in our concentration range, $(D_{21})_V/(D_{22})_V$ is also closely approximated by the thermodynamic ratio μ_{21}/μ_{22} . We also expect that $(D_{21})_0/(D_{22})_0$ will be close to μ_{21}/μ_{22} for a broad class of ternary systems in which a macromolecular polyelectrolyte has a large molar volume and a small concentration with respect to a salt having a common ion.

The expression relating the μ_{ij} (eq 8 of ref 7), can be solved for μ_{21}/μ_{22} giving

$$\frac{\mu_{21}}{\mu_{22}} = \frac{\mu_{12}}{\mu_{22}} \frac{1 - C_2 \bar{V}_2}{1 - C_1 \bar{V}_1} + \frac{C_2 \bar{V}_1}{1 - C_1 \bar{V}_1} - \frac{\mu_{11}}{\mu_{22}} \frac{C_1 \bar{V}_2}{1 - C_1 \bar{V}_1} \quad (14)$$

Examining the magnitudes of the various terms for NaCl (6,7), NH_4Cl (7), and KCl (Table 1), we find that \bar{V}_2 varies between 0.018 and 0.038 $\text{dm}^3 \text{mol}^{-1}$ at $C_1 = 0.6$ mM. Therefore,

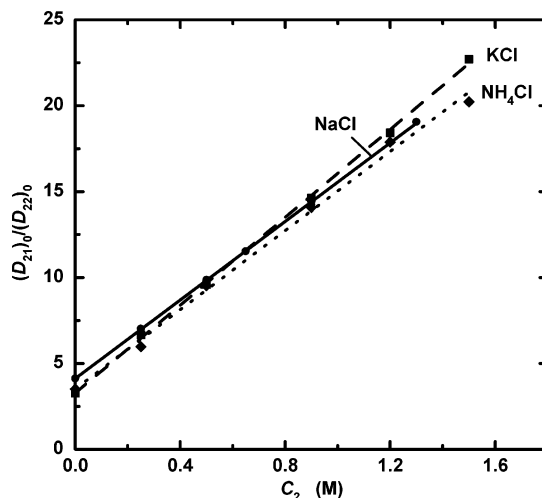


Figure 4. The ratio $(D_{21})_0/(D_{22})_0$ as a function of MCl concentration, C_2 , at pH 4.5 and 25 °C: ●, M = Na; ■, M = K; ◆, M = NH_4 . The curves (—, M = Na; ---, M = K; ···, M = NH_4) are linear fits to the data. They yield: $z_p/2 = 4.1, 3.5$, and 3.3 for NaCl, NH_4Cl , and KCl, respectively, at $C_2 = 0$, consistent with the z_p values tabulated in Table 3. Slopes $(\omega + \bar{V}_1)$ for the three salts are 11.4, 11.5, and 12.8 M^{-1} , respectively. Corresponding plots (not shown) of $(D_{21})_V/(D_{22})_V$ exhibit similar behavior.

the results in Tables 1 and 2 show that the third term of the right-hand side (RHS) is very small compared to the others (not exceeding about 1% of their sum). Consequently, it is an excellent approximation to ignore this term.

The second term on the RHS of eq 14 essentially accounts for the difference between μ_{21} and μ_{12} and is equal to $-(\partial C_2 / \partial C_1)_{m_2}$ where m_2 is the molality of the salt.²³ This quantity describes the change of the molar concentration of the salt, since addition of lysozyme chloride at constant m_2 (i.e., at constant salt/solvent ratio) increases the total volume of the system. Importantly, the significant increase in total volume is due to the large volume of the lysozyme molecules. In this case, m_2 characterizes the composition of the saltwater medium surrounding the large protein molecules better than C_2 does.

To examine the dependence of μ_{21}/μ_{22} on C_2 , we note that the $C_i \bar{V}_i$ terms are small compared to unity. Therefore, we can approximate the first term of the RHS of eq 14 by μ_{21}/μ_{22} and the second term by $C_i \bar{V}_i$. From eq 6, we can write, in the limit $z_p C_1 \ll C_2$

$$\frac{\mu_{12}}{\mu_{22}} = \frac{z_p + C_2(z_p + 1)(\partial \ln y_1 / \partial C_2)}{2[1 + C_2(\partial \ln y_2 / \partial C_2)]} \quad (15)$$

Our experimental data show that μ_{12}/μ_{22} can be roughly approximated by the linear relation $z_p/2 + \omega C_2$, where $\omega > 0$ accounts for the effect of salt on the lysozyme chloride activity coefficient. Furthermore, $\bar{V}_1 \approx 10.2 \text{ dm}^3 \text{mol}^{-1}$, nearly independent of salt and salt concentration. Therefore, the second term on the RHS of eq 14 is proportional to C_2 . Consequently

$$\frac{(D_{21})_0}{(D_{22})_0} \approx \frac{\mu_{21}}{\mu_{22}} \approx \frac{z_p}{2} + (\omega + \bar{V}_1)C_2 \quad (16)$$

To understand the physical basis of eq 16, we first note that the intercept $z_p/2$ is related to the electrostatic coupling between protein and salt. Indeed, the intercept can be directly obtained using relations for D_{21} and D_{22} shown in eq 10. We also observe that \bar{V}_1 is responsible for more than 80% of $\omega + \bar{V}_1$, the slope of $(D_{21})_0/(D_{22})_0$. This is again due to the large volume of the

lysozyme molecules. The near constancy of \bar{V}_1 and the approximately linear variation of μ_{12}/μ_{22} with C_2 for each salt jointly explain why over our concentration range the three $(D_{21})_0/(D_{22})_0$ curves differ, to a good approximation, by only an additive constant (see Figure 4). The small offsets are due to differences in the constant term $z_p/2$ in eq 16.

For ternary solutions involving one large solute, a $(D_{21})_V$ larger than that calculated from a purely N-H analysis can be qualitatively explained using excluded volume concepts. Consider a solution in which the salt has a uniform stoichiometric concentration C_2 and a macromolecule has a concentration gradient. Because the macromolecules occupy space in the solution, the "effective" salt concentration in the interstitial volume surrounding them will exceed the stoichiometric value C_2 and will increase as the protein concentration increases along its gradient. Therefore, in such a lysozyme chloride-saltwater solution with no gradient of the stoichiometric salt concentration C_2 , a gradient of lysozyme chloride will produce an "effective gradient" of salt in the same direction. This resulting effective concentration gradient of salt will drive a salt flux and lead to increases to the (already positive) values of $(D_{21})_0$ and $(D_{21})_V$.

Thermodynamic and Crystal Growth Applications. Here, we consider the implications of the reported measurements, as well as overall approaches for several problems of interest.

Protein Solubility. Lysozyme is one of several proteins for which chloride salts are good precipitants,⁴⁵ so that understanding how the relevant thermodynamic properties depend on the nature and concentration of the three salts is of direct interest. Here, we show how the μ_{12} dependence on salt concentration can be used to establish the dependence of protein solubility on salt concentration, $S_1(C_2)$.

At equilibrium, the protein chemical potential in the liquid phase, μ_1 , is equal to the protein chemical potential in the solid phase, μ_1^s . The variation of protein solubility with salt concentration is given by $d\mu_1^s = d\mu_1 = \mu_{11} dC_1 + \mu_{12} dC_2$. Therefore, at equilibrium ($S_1 = C_1$)

$$(dS_1/dC_2) = -(\mu_{12}/\mu_{11}) + (d\mu_1^s/dC_2)/\mu_{11} \quad (17)$$

To first order with respect to the protein concentration C_1 , we have $\mu_{11}/(RT) = [1 + O(C_1)]/C_1$ and $\mu_{12}/(RT) = z_p/C_2 + a_{12} + b_{12}C_2 + O(C_1)$. Since $S_1 = C_1$ at equilibrium, we obtain

$$(d \ln S_1/dC_2) = -(z_p/C_2) - a_{12} - b_{12}C_2 + (d\mu_1^s/dC_2)/RT \quad (18)$$

It is usually assumed that the solid protein either is a pure crystalline phase or at least contains no salt. However, as earlier, we have so far made no assumptions about the solid phase of the protein other than that its properties are independent of the nature and concentration of the salt, i.e., $d\mu_1^s = 0$. In that case, the slope of the logarithm of the solubility, $d \ln S_1/dC_2$, would be approximately equal to $-\mu_{12}/(RT)$, and thus

$$(d \ln S_1/dC_2) = -(z_p/C_2) - a_{12} - b_{12}C_2 \quad (19)$$

We now address the issue of how our values of μ_{12} obtained at $C_1 = 0.6$ mM can be used to test eq 19. We expect that if the solubility of the protein is small with respect to the salt concentration within the experimental range of interest ($C_2 \geq 0.25$ M), then μ_{12} will not significantly depend on C_1 .

Slopes calculated from lysozyme chloride solubility measurements in aqueous NaCl^{32,46,47} are only about 25% of those predicted from our μ_{12} values. This percentage is estimated to be at most 30% when the predicted values include terms higher

order in C_1 in the expression for μ_{11} . Thus, the approximation $\mu_{11}/(RT) = 1/C_1$ does not account for the large difference between $d \ln S_1/dC_2$ and $-\mu_{12}/(RT)$. These results thus imply that the approximation $d\mu_1^s = 0$ is not valid. Since $d \ln S_1/dC_2 > -\mu_{12}/(RT)$ (eq 19), we conclude that μ_1^s increases as C_2 increases.

We now qualitatively discuss the behavior of $\mu_1^s(C_2)$. It has been experimentally found that marked salt repartitioning between the liquid and the solid phase occurs.^{48,49} Since small ions penetrate into the solid phase, Donnan equilibrium will be established between the solution and the crystal "channels" as discussed by Warren.⁵⁰ Due to the large amount of protein cations inside the solid phase, an excess of chloride anions⁵¹⁻⁵³ will be responsible for crystal electroneutrality as in the case of polyelectrolyte gels. Thus, the chemical potential of the protein component, μ_1^s , is expected to increase with the solid-phase concentration of chloride ions, which, in turn, increases with C_2 due to repartitioning. That the analysis of the (liquid-phase) μ_{12} values correctly predicts the Hofmeister series of solubilities suggests that, although μ_1^s is in fact a function of the salt concentration, the effects of the salt *type* on μ_1^s are too small to affect the Hofmeister solubility ordering. On the other hand, quantitative prediction of solubility has not yet been realized.

We now discuss the implications of eq 19 with a commonly used solubility relationship. At relatively high salt concentrations, the dependence of protein solubility on salt concentration is commonly approximated by^{32,54}

$$\ln S_1 = A - KC_2 \quad (20)$$

where $K > 0$ is the salting-out constant. Equation 20 neglects the Debye-Huckel square-root term, which affects the solubility only at very low salt concentrations.

However, integration of eq 18 with respect to C_2 gives four terms: a constant and terms linear, quadratic, and logarithmic in C_2 . Since we have found that z_p/C_2 is a large contributor to μ_{12} , we expect that a $z_p \ln C_2$ contribution from the common-ion effect should be very significant. Interestingly, plots of $\ln S_1$ vs $\ln C_2$ are significantly more linear than those of $\ln S_1$ vs C_2 reported in refs 32, 46, and 47 (based on eq 20).

Parts a and b of Figure 5 show plots of solubility data from ref 40, using eq 20 and the equation

$$\ln S_1 = \hat{A} - \hat{K} \ln C_2 \quad (21)$$

respectively, with the parameters determined in each case by linear least squares. We considered only data satisfying $S_1 \ll C_2$, for which the approximation $\mu_{11}/(RT) = 1/C_1$ is valid. The plots, correlation coefficients, and root-mean square errors all show that eq 21 gives a significantly more linear relationship, and hence better represents the data, than does eq 20. We find similar improvement for other solubility data.^{46,47}

We suggest that, in the case of a highly charged macroion such as the lysozyme cation at pH values far from the isoelectric point, eq 21 describes the dependence of the solubility of the macromolecular component on salt concentration better than eq 20 does. This is corroborated not only by the dependence of protein solubility on salt concentration but also on the dependence of \hat{K} on pH. If we examine solubility data of lysozyme³² at different pH values using eq 21, we conclude that \hat{K} increases as pH decreases away from the isoelectric point. This is consistent with a corresponding increase of lysozyme net charge. This has important implications on the pH dependence of protein solubility at constant salt concentration. It is generally expected

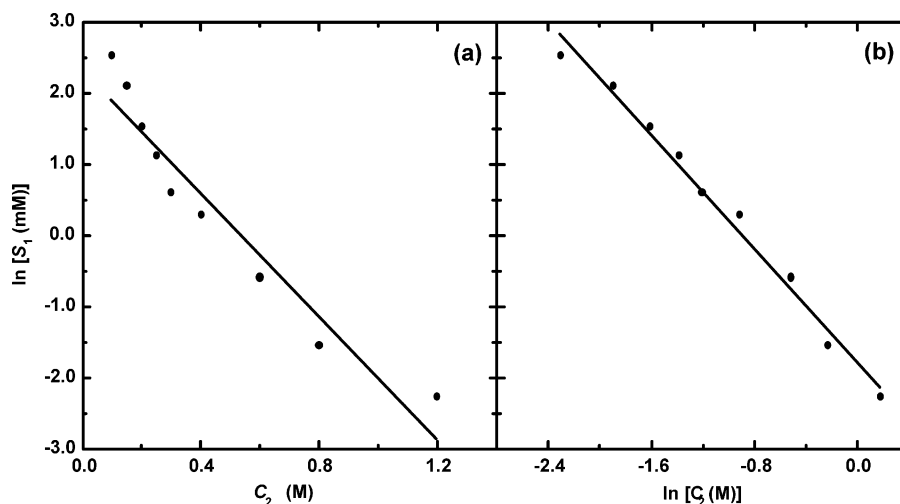


Figure 5. Semilogarithmic (a) and logarithmic (b) plots of lysozyme chloride solubility, S_1 , vs NaCl concentration, C_2 , at 18 °C and pH = 4.3. The data are taken from Retailleau et al.,³² to which the lines are fitted by least squares ($r^2 = 0.929$ and 0.988 , and root mean square deviations of 0.463 and 0.194 for the semilogarithmic and logarithmic plots, respectively).

that protein solubility monotonically increases as pH moves away from the isoelectric point, due to a corresponding increase of the protein net charge.^{29,31} As shown by Retailleau et al.,³² this is true for lysozyme only at low NaCl concentration. Indeed, at high NaCl concentration ($C_2 > 0.6$ M), lysozyme solubility decreases as pH decreases from 8.7 to 3.3.³² This inversion is a consequence of the pH dependence of \bar{K} . Thus our results are consistent with the experimental evidence that protein solubility can decrease even when the protein net charge increases (at constant salt concentration).

Salt Ion Insertion in Crystals. We speculate that the magnitude and sign of $(D_{21})_V$ may have implications for crystal growth under diffusion control. At the solid–liquid interface, precipitation of protein induces a protein concentration gradient between the interface and the bulk solution, which in turn will drive a flux of salt toward the crystal.⁵⁵ This can enhance salt ion insertion into the solid phase. Salt ions in the interior can significantly affect the morphology of protein crystals⁵² and might ultimately be responsible for compromising crystal chemical and mechanical properties, and hence crystal quality.⁴⁹ On the other hand, for the small values of $(D_{12})_V$ reported here, there is little protein backflux from the induced salt gradient. However, the small increase in salt concentration at the surface will increase the degree of supersaturation, which is the driving force for crystal growth. We note that at the high salt concentrations relevant to crystal growth, transport of salt to the interface, and the resulting change in salt concentration there, has very little effect on the numerical values of the multicomponent diffusion coefficients $(D_{ij})_V$, as shown in Figure 1.

Implications for Nucleation and Cluster Dynamics. The coefficient $(D_{12})_V$ might play a significant role in protein crystal growth. Initial clustering of lysozyme cations will increase the protein concentration and decrease the salt and water concentrations in the volume of the cluster. If one considers the lysozyme chloride flux (eq 1), a positive $(D_{12})_V$ will contribute to a protein flux toward the cluster interior. This will tend to counter the effects of the positive $(D_{11})_V$ term that drives a flux of lysozyme chloride away from the interior of the cluster. While direct quantitative application of the macroscopic Fick's law to microscopic systems is questionable, the *direction* of the counterflux predicted by this argument would seem to be correct, at least for an ensemble of clusters. This suggests that in a series of aqueous salt solutions of a protein, larger values of $(D_{12})_V/(D_{11})_V$ at supersaturation increase the likelihood that protein will

be transported to the cluster and that nucleation will occur. It is interesting to note that NaCl has been the precipitant that works well for lysozyme and is used commercially, and that of the three salts considered NaCl has the highest ratio $(D_{12})_V/(D_{11})_V$ at nucleation conditions.

Thermodynamics of Hydrated Proteins. When a protein precipitates, considerable water is usually included in the solid phase, with the mass fraction of water being 30–40% for lysozyme (depending on crystal habit) and in the range of 25–65% for other proteins.⁵⁶ In addition, salt ions, other small molecules, or larger molecules (including other proteins or other polyelectrolytes) are frequently included in the solid phase. Some included small molecules (e.g., water) are sometimes associated with particular sites in the protein,^{51,52} while other species are included more irregularly, possibly “in solution” in “included water”.

As noted above, included species are expected to affect the protein chemical potential in the solid phase and hence the chemical potential of protein in the aqueous phase with which it is in equilibrium. Our technique for acquiring relatively high precision thermodynamic data in “asymmetric” multicomponent solutions,⁷ especially in the supersaturated region, together with solubility data, opens the door to better understanding the thermodynamics of hydrated protein crystals and, more generally, of protein crystals that include other species.

Conclusions

For lysozyme chloride in aqueous salt solutions at pH 4.5 and 25 °C, we have shown that the common-ion effect dominates the chemical potential derivatives at low salt concentration and still accounts for about 50% of μ_{12} even at the highest concentrations considered, contrary to common belief.

We have discussed the values of $\mu_{12}^{(m)}$ for the three salts and shown that the chemical potential $\mu_1(C_2)$ increases in the sequence $\text{NH}_4\text{Cl} < \text{KCl} < \text{NaCl}$, consistent with the order of the Hofmeister series. The results indicate that liquid- and solid-phase lysozyme chlorides are at equilibrium at salt concentrations that increase in the order NaCl, KCl, NH_4Cl .

That the common-ion contribution dominates the dependence of the protein chemical potential on salt concentration has important implications for salt effects on protein solubility. It provides a $\ln C_2$ term to the $\ln S_1$ expression. Indeed, we have

suggested that, for a highly charged protein such as lysozyme, $\ln S_1 = \hat{A} - \hat{K} \ln C_2$ should describe the behavior of the solubility better than $\ln S_1 = A - KC_2$. Moreover, by comparing $d \ln S_1/dC_2$ and our values of μ_{12}/RT , we have deduced that the protein chemical potential in the solid phase depends significantly on salt concentration. This is consistent with the capability of protein crystals to accommodate salt ions and indicates that salt concentration plays a crucial role in crystal quality.

We have demonstrated the predictability of $(D_{11})_V$ and $(D_{22})_V$ and developed a basic understanding of the relation of these main-term diffusion coefficients to chemical potential derivatives. For each salt, the dependence of $(D_{11})_V$ on salt concentration correlates with the concentration dependence of the viscosity of the binary salt solution. At each salt concentration, values of $(D_{11})_V \eta/\eta_0$ are similar for NaCl and KCl but are larger for solutions in NH_4Cl . The least predictable diffusion coefficients are $(D_{12})_V$ and the derived $(D_{12})_0$. At low salt concentrations, long-range electrostatic effects can account for the salt-specific differences in their dependence on salt concentration. Our thermodynamic analysis demonstrates that the concentration dependence of $(D_{21})_0/(D_{22})_0$ (and hence $(D_{21})_V/(D_{22})_V$) is primarily related to the large molar volume of the protein. We show that an appropriate extrapolation of this quotient versus salt concentration from measurements made for $C_1 \ll C_2$ yields about one-half the protein charge, $z_p/2$.

We suggest how the cross-diffusion coefficients may play a role in crystallization kinetics, with salt-ion insertion into the crystalline phase being enhanced during crystal growth due the magnitude and sign of $(D_{21})_V$. The other cross-coefficient, $(D_{21})_V$, might be important in initial clustering of lysozyme cations during nucleation.

Acknowledgment. The support of the NASA Microgravity Biotechnology Program through Grant NAG8-1356 is gratefully acknowledged. A small portion of the work of D.G.M. was performed under the auspices of the U.S. Department of Energy, Office of Basic Energy Sciences, at Lawrence Livermore National Laboratory, under Contract No. W-7405-ENG-48.

Supporting Information Available: Experimental details on the determination of ternary diffusion coefficients and tables of experimental ternary diffusion results. This material is available free of charge via the Internet at <http://pubs.acs.org>.

References and Notes

- Arakawa, T.; Bhat, R.; Timasheff, S. N. *Biochemistry* **1990**, *29*, 1914.
- Timasheff, S. N.; Xie, G. *Biophys. Chem.* **2003**, *105*, 421.
- Courtneay, E. S.; Capp, M. W.; Anderson, C. F.; Record, M. T., Jr. *Biochemistry* **2000**, *39*, 4455.
- Curtis, R. A.; Ulrich, J.; Montaser, A.; Prausnitz, J. M.; Blanch, H. W. *Biotechnol. Bioeng.* **2002**, *79*, 367.
- Görlich, D.; Mattaj, I. W. *Science* **1996**, *271*, 1513.
- Albright, J. G.; Annunziata, O.; Miller, D. G.; Paduano, L.; Pearlstein, A. J. *J. Am. Chem. Soc.* **1999**, *121*, 3256.
- Annunziata, O.; Paduano, L.; Pearlstein, A. J.; Miller, D. G.; Albright, J. G. *J. Am. Chem. Soc.* **2000**, *122*, 5916.
- Paduano, L.; Annunziata, O.; Pearlstein, A. J.; Miller, D. G.; Albright, J. G. *J. Cryst. Growth* **2001**, *232*, 273.
- Gilliland, G. L.; Ladner, J. E. *Curr. Opin. Struct. Biol.* **1996**, *6*, 595.
- Santesson, S.; Cedergren-Zeppeauer, E. S.; Johansson, T.; Laurell, T.; Nilsson, J.; Nilsson, S. *Anal. Chem.* **2003**, *75*, 1733.
- Roe, S. *Protein Purification Techniques*; Oxford University Press: Oxford, 2001.
- Blanch, H. W.; Prausnitz, J. M.; Curtis, R. A.; Bratko, D. *Fluid Phase Equilib.* **2002**, *194*, 31.
- George, A.; Wilson, W. W. *Acta Crystallogr.* **1994**, *D50*, 361.
- Saksena, S.; Zydney, A. L. *J. Membr. Sci.* **1997**, *125*, 93.
- Kirkwood, J. G.; Baldwin, R. L.; Dunlop, P. J.; Gosting, L. J.; Kegeles, G. J. *Chem. Phys.* **1960**, *33*, 1505.
- Dunlop, P. J.; Gosting, L. J. *J. Phys. Chem.* **1959**, *63*, 86.
- Woolf, L. A.; Miller, D. G.; Gosting, L. J. *J. Am. Chem. Soc.* **1962**, *84*, 317.
- Miller, D. G.; Vitagliano, V.; Sartorio, R. *J. Phys. Chem.* **1986**, *90*, 1509.
- Canfield, R. E. *J. Biol. Chem.* **1963**, *238*, 2698.
- Tanford, C.; Wagner, M. L. *J. Am. Chem. Soc.* **1954**, *76*, 3331.
- Miller, D. G.; Albright, J. G.; Mathew, R.; Lee, C. M.; Rard, J. A.; Eppstein, L. B. *J. Phys. Chem.* **1993**, *97*, 3885.
- Fujita, H.; Gosting, L. J. *J. Am. Chem. Soc.* **1956**, *78*, 1099.
- Miller, D. G. *J. Phys. Chem.* **1959**, *63*, 570.
- Piazza, R.; Pierno, M. J. *Phys.: Condens. Matter* **2000**, *12*, A443.
- Guo, H.; Kao, S.; McDonald, H.; Asanov, A.; Combs, L. L.; Wilson, W. W. *J. Cryst. Growth* **1999**, *196*, 424.
- Arakawa, T.; Timasheff, S. N. *Biochemistry* **1984**, *23*, 5912.
- We analyze the two cross derivatives based on molarity because, as we shall see later, they allow us to discuss some important aspects of the four diffusion coefficients.
- Miller, D. G. *J. Phys. Chem.* **1966**, *70*, 2639.
- Tanford, C. *Physical Chemistry of Macromolecules*; Wiley: New York, 1961.
- Annunziata, O. Ph.D. dissertation, Texas Christian University, 2001.
- Arakawa, T.; Timasheff, S. N. *Methods Enzymol.* **1985**, *114*, 49.
- Retailleau, P.; Riès-Kautt, M.; Ducruix, A. *Biophys. J.* **1997**, *73*, 2156.
- Riès-Kautt, M.; Ducruix, A. *J. Biol. Chem.* **1989**, *264*, 745.
- Riès-Kautt, M.; Ducruix, A. *J. Cryst. Growth* **1991**, *110*, 20.
- Riès-Kautt, M.; Ducruix, A. *Methods Enzymol.* **1997**, *276*, 23.
- Tardieu, A.; Finet, S.; Bonnete, F. *J. Cryst. Growth* **2001**, *232*, 1.
- Finet, S.; Skouri-Panet, F.; Casselyn, M.; Bonnete, F.; Tardieu, A. *Curr. Opin. Colloid Interface Sci.* **2004**, *9*, 112.
- We use the subscript "1" for the protein component and the subscript "2" for the salt component, consistent with the literature on multicomponent diffusion. However, the subscript "2" for the protein component and the subscript "3" for the salt component are extensively used in relation to the thermodynamic description of ternary mixtures.
- Robinson, R. A.; Stokes, R. H. *Electrolyte Solutions*; Academic Press: New York, 1955.
- Gosting, L. J. *Adv. Protein Chem.* **1956**, *11*, 429.
- Gosting, L. J.; Harned, H. S. *J. Am. Chem. Soc.* **1951**, *73*, 159.
- Zhang, H.-L.; Han, S.-J. *J. Chem. Eng. Data* **1996**, *41*, 516.
- Della Monica, M.; Ceglie, A.; Agostiano, A. *Electrochim. Acta* **1984**, *29*, 933.
- Miller, D. G. *J. Phys. Chem.* **1967**, *71*, 616.
- Gilliland, G. L. *J. Cryst. Growth* **1988**, *90*, 51.
- Howard, S. B.; Twigg, P. J.; Baird, J. K.; Meehan, E. J. *J. Cryst. Growth* **1988**, *90*, 94.
- Forsythe, E. L.; Judge, R. A.; Pusey, M. L. *J. Chem. Eng. Data* **1999**, *44*, 637.
- Palmer, K. J.; Ballantyne, M.; Galvin, J. A. *J. Am. Chem. Soc.* **1948**, *70*, 906.
- Vekilov, P. G.; Monaco, L. A.; Thomas, B. R.; Stojanoff, V.; Rosenberger, F. *Acta Crystallogr.* **1996**, *D52*, 785.
- Warren, P. B. *J. Phys.: Condens. Matter* **2002**, *14*, 7617.
- Vaney, M. C.; Maignan, S.; Riès-Kautt, M.; Ducruix, A. *Acta Crystallogr.* **1996**, *D52*, 505–517.
- Vaney, M. C.; Broutin, I.; Retailleau, P.; Douangamath, A.; Lafont, S.; Hamiaux, C.; Prange, T.; Ducruix, A.; Riès-Kautt, M. *Acta Crystallogr.* **2001**, *D57*, 929.
- The presence of small-ion sites inside lysozyme crystals been shown by X-ray diffraction (see ref 52 and references therein). In the case of chloride anions, only one specific site was clearly identified (see ref 51 and references therein). It is likely that most chloride ions show nonspecific interactions with the surface of lysozyme molecules.
- Cohn, E. J. *Physiol. Rev.* **1925**, *5*, 349.
- Annunziata, O.; Albright, J. G. *Ann. N. Y. Acad. Sci.* **2002**, *974*, 610.
- Matthews, B. W. *J. Mol. Biol.* **1968**, *33*, 491.
- Rard, J. A.; Miller, D. G. *J. Solution Chem.* **1979**, *8*, 701.
- Rard, J. A.; Miller, D. G. *J. Chem. Eng. Data* **1980**, *25*, 211.
- Albright, J. G.; Mitchell, J. P.; Miller, D. G. *J. Chem. Eng. Data* **1994**, *39*, 195.